

# EphrinB2 activation enhances angiogenesis, reduces amyloid- $\beta$ deposits and secondary damage in thalamus at the early stage after cortical infarction in hypertensive rats

Shihui Xing<sup>1</sup>, Nannan Pan<sup>2</sup>, Wei Xu<sup>1</sup>, Jian Zhang<sup>1</sup>, Jingjing Li<sup>1</sup>, Chao Dang<sup>1</sup>, Gang Liu<sup>1</sup>, Zhong Pei<sup>1</sup> and Jinsheng Zeng<sup>1</sup>

## Abstract

Cerebral infarction causes secondary neurodegeneration and angiogenesis in thalamus, which impacts functional recovery after stroke. Here, we hypothesize that activation of ephrinB2 could stimulate angiogenesis and restore the secondary neurodegeneration in thalamus after cerebral infarction. Focal cerebral infarction was induced by middle cerebral artery occlusion (MCAO). Secondary damage, angiogenesis, amyloid- $\beta$  (A $\beta$ ) deposits, levels of ephrinB2 and receptor for advanced glycation end product (RAGE) in the ipsilateral thalamus were determined by immunofluorescence and immunoblot. The contribution of ephrinB2 to angiogenesis was determined by siRNA-mediated knockdown of ephrinB2 and pharmacological activation of ephrinB2. The results showed that formation of new vessels and ephrinB2 expression was markedly increased in the ipsilateral thalamus at seven days after MCAO. EphrinB2 knockdown markedly suppressed angiogenesis coinciding with increased A $\beta$  accumulation, neuronal loss and gliosis in the ipsilateral thalamus. In contrast, clustered EphB2-Fc significantly enhanced angiogenesis, alleviated A $\beta$  accumulation and the secondary thalamic damage, which was accompanied by accelerated function recovery. Additionally, activation of ephrinB2 significantly reduced RAGE levels in the ipsilateral thalamus. Our findings suggest that activation of ephrinB2 promotes angiogenesis, ameliorates A $\beta$  accumulation and the secondary thalamic damage after cerebral infarction. Additionally, RAGE might be involved in A $\beta$  clearance by activating ephrinB2 in the thalamus.

## Keywords

Amyloid, angiogenesis, cerebral infarction, secondary damage, thalamus

Received 4 November 2017; Accepted 14 March 2018

## Introduction

Focal cerebral infarction causes secondary neuronal degeneration in the ipsilateral thalamus as a resultant of cortical disconnection, accounting for somatosensory and even cognitive impairment.<sup>1,2</sup> Increasing evidence shows that thalamic pathology secondary to cerebral infarction involves retrograde axonal degeneration, inflammation, oxidative stress and neuroregenerative inhibitory factors (such as Nogo-A).<sup>3–6</sup> Recent studies have further showed that cerebral ischemia leads to progressive amyloid- $\beta$  (A $\beta$ ) aggregation in the thalamus, which relates to the secondary thalamic neurodegeneration.<sup>7–10</sup> Moreover, blockade of A $\beta$  production can

reduce the neuronal injury in thalamus following ischemic stroke.<sup>11,12</sup> These findings suggest a similar pathogenesis shared by secondary thalamic neurodegeneration after stroke and Alzheimer's disease (AD).

<sup>1</sup>Department of Neurology and Stroke Center, The First Affiliated Hospital, Sun Yat-Sen University, Guangzhou, China

<sup>2</sup>Department of Neurology, The Affiliated Brain Hospital of Guangzhou Medical University, Guangzhou, China

## Corresponding authors:

Shihui Xing and Jinsheng Zeng, Stroke Center and Department of Neurology, The First Affiliated Hospital, Sun Yat-Sen University, No. 58 Zhongshan Road 2, Guangzhou 510080, China.

Email: xingshuh@mail.sysu.edu.cn; zengjs@pub.guangzhou.gd.cn

Cerebral infarction triggers a process of neurogenesis and angiogenesis in the peri-infarct areas and subventricular zone.<sup>13</sup> Recent studies have shown that cerebral infarction also induces newly formation of vascular network and angiogenesis in the thalamus remote from focal cerebral infarction.<sup>14,15</sup> Angiogenesis after ischemic stroke may function the repair mechanisms by removing the detrimental factors or even damaged tissues. Evidence of studies in AD has shown that insufficient angiogenesis might link to the pathological A $\beta$  aggregation.<sup>16</sup> Taken these above findings, strategies for enhancing angiogenesis might have potentials for protecting the secondary thalamic damage against A $\beta$  aggregation after stroke. However, the mechanisms underlying angiogenesis in the thalamus after stroke remain unclear.

EphrinB ligands and their cognate Eph receptors are one of the most important guidance molecules that play diverse roles in axon guidance, neuronal plasticity, spine maturation, and synaptogenesis in a bidirectional fashion.<sup>17</sup> In vascular development, the ephrinB2 ligand and its receptor EphB4 have been shown to specifically express on arterial and venous endothelial cells and govern the cardiovascular development in the embryo.<sup>18,19</sup> Targeted inactivation of ephrinB2 genes in mice leads to disruption of embryonic vessel formation and causes early lethality.<sup>20</sup> Consistently, endothelial specific deletion of ephrinB2 results in defects in vascular morphogenesis.<sup>21</sup> In contrast, functional ephrinB2 expression has been shown to promote interactions between arterial and venous vessels in postnatal neovascularization.<sup>22</sup> In addition, increased expression of ephrinB2 enhanced vessel pruning and pericytes-to-endothelial assembly during vascular remodeling.<sup>23,24</sup> Whereas the critical roles of ephrinB2 in angiogenesis and vascular patterning have been widely investigated, very little is known whether ephrinB2 regulates postnatal angiogenesis in the thalamus after distal cerebral infarction. Also, it remains unclear whether ephrinB2-mediated angiogenesis impacts the secondary thalamic damage after cerebral infarction.

The present study was designed to investigate the alterations of ephrinB2 expression and the effects of ephrinB2 activation on angiogenesis in the ipsilateral thalamus after focal cerebral infarction. Further, we sought to determine the possible effects of ephrinB2-mediated angiogenesis on A $\beta$  accumulation and the secondary neurodegeneration in the ipsilateral thalamus after focal cerebral infarction.

## Material and methods

### Animal models and experimental groups

The stroke-prone renovascular hypertensive rats (RHRSP) model was established in male Sprague-Dawley rats weighing 80–100 g using a two kidney, two-clip method as

previously described.<sup>25</sup> Animals were housed under a 12-h light/dark cycle and had ad libitum access to water and laboratory diet. The experimental protocol was approved by the Institutional Animal Ethical Committee of Sun Yat-Sen University and conducted according to the Guide for the Care and Use of Laboratory Animal of the National Institute of Health in China. Reporting of this study complies with the ARRIVE (Animal Research: Reporting in vivo Experiments) guidelines.

The experimental groups were randomly assigned in a blind manner. Firstly, a group of RHRSP was randomly assigned to MCAO or sham surgery (12 animals each group) as described previously with minor modifications.<sup>26</sup> Briefly, under anesthesia with 10% chloral hydrate (3 ml/kg body weight), a vertical incision was made midway between the lateral canthus of the right eye and the right external auditory canal. The right temporalis muscles were separated and retracted inferiorly downward to expose the zygomatic and squamosal bone. Under an operating microscope, a 3-mm burr hole was drilled 2–3 mm rostral to the fusion of the zygomatic arch with the squamosal bone to expose the right middle cerebral artery (MCA), and the craniotomy was then extended dorsally up to the first major branch of the right MCA. The dura was gently opened with a bent 24-gauge needle and the right MCA was occluded distal to the origin of the striatal branches using bipolar electrocoagulation. Animals subjected to sham surgery were treated similarly except for occlusion of the MCA. Secondly, another group of RHRSP randomly received a stereotactically guided intrathalamic injection of lentivirus-mediated ephrinB2 shRNA vector (referred to as *Efnb2*-shRNA) or lentivirus vector carrying scrambled shRNA (referred to as Scramble-shRNA) at 10 weeks after renovascular hypertension surgery and then underwent unilateral MCAO surgery at 14 days after injection (12 animals each group) as previously described.<sup>27</sup> Thirdly, additional group of RHRSP underwent MCAO and were randomly selected for intraventricular injection of clustered EphB2-Fc or IgG-Fc at 24 h after MCAO (12 animals each group). Body temperature of animals was kept at  $37 \pm 0.5^\circ\text{C}$  with a heating pad during the surgery and recovery periods. In total, 12 animals in various groups were excluded. Reasons were failure to establish MCAO (six animals without motor deficit at 24 h post-operation), intracranial hemorrhage (two animals) or death due to anesthesia during intracranial injection (two in *Efnb2*-shRNA, one in Scramble-shRNA and one in IgG-Fc groups respectively).

### Lentiviral construction preparation and intrathalamic injection

Four shRNA sequences targeting rat ephrinB2 and one negative control sequence were constructed by

Genechem (Shanghai). The best-performing-siRNA sequence was *AAGCCGACAGATGCACTATTA*, and the negative control scrambled siRNA sequence was *TTCTCCGAACGTGTCACGT*. siRNAs were inserted into a pFU-GW-siRNA lentivirus vector containing a CMV-driven EGFP reporter gene and an U6 promoter upstream of restriction sites (Hpa I and Xho I) (Genechem). Recombinant lentiviruses were produced by co-transfecting 293T cells with the aid of Lipofectamine 2000 (Invitrogen) according to standard protocols. Virus titers, expressed as transducing units (TU) per milliliter, were determined by measuring GFP expression in 293T cells, which were transduced with serial dilutions of concentrated lentivirus. The titers were approximately  $1.2 \times 10^9$  TU/ml. Lentivirus preparations were infused stereotactically into the right thalamus region. Briefly, RHRSP were anesthetized as above and shRNA preparations were delivered into the right thalamus using a 25- $\mu$ l Hamilton syringe at the following coordinates (4 injection sites, 3- $\mu$ l per site): -2.6 mm anteroposterior, 2.6 mm lateral, -6.4/-6.6 mm dorsoventral; -3.0 mm anteroposterior, 2.8 mm lateral, -6.2/-6.4 mm dorsoventral relative to bregma via a stereotactic apparatus. The animals were allowed to recover for up to 14 days to enable sufficient gene expression.

#### *Intraventricular administration of clustered EphB2-Fc and IgG-Fc*

To determine the effects of ephrinB2 activation on angiogenesis in the thalamus, recombinant EphB2-Fc protein (R&D) consists of the Fc domain of human IgG1 (Fc) linked to the ectodomain of EphB2 receptor, which lacks the tyrosine kinase domain implicated in signal transduction and blocks EphB signaling by binding available ligands, but can also activate ephrinB2 ligands in a clustered manner.<sup>28-30</sup> Recombinant EphB2-Fc or IgG-Fc was diluted in 0.01 M phosphate-buffered saline (PBS, pH7.4) containing 0.1% human serum albumin (200  $\mu$ g/ml) and pre-clustered by incubation with anti-human Fc $\gamma$  (Jackson Immunoresearch Laboratories) at a ratio of 10:1 for 2 h at room temperature. Pre-clustered EphB2-Fc and IgG-Fc were administered into lateral ventricle at 24 h post-MCAO for consecutive three days. Briefly, a dose of 100  $\mu$ l of pre-clustered EphB2-Fc or IgG-Fc was administered stereotactically into the right lateral ventricle via osmotic minipumps (Alzet 100ul, Alza Scientific Products) at coordinates: -1.0 mm anteroposterior, 1.4 mm lateral, -4.0 mm dorsoventral relative to bregma.

#### *Bromodeoxyuridine labeling*

To labeling the dividing endothelial cells, bromodeoxyuridine (BrdU) (BB9285; Sigma-Aldrich) was

dissolved in 0.9% sodium chloride and intraperitoneally injected (50 mg/kg) in all groups at 8 h intervals twice daily for six consecutive days at 24 h after MCAO. This allowed us to investigate the cumulative proliferation and phenotype pattern of cells after cerebral infarction.

#### *Behavioral test*

Adhesive removal test was performed by an experimenter blind to the study design to assess the somatosensory deficits at seven days after MCAO as previously described.<sup>31</sup> Briefly, two small pieces of adhesive paper dots (113.1 mm<sup>2</sup>) were attached to the distal-radial region on the wrist of each forelimb. The time to remove each stimulus from the forelimbs was recorded in five trials per day at an interval of at least 5 min between trials. Animals were trained for three consecutive days to remove the dots within 10 s prior to MCAO surgery. The mean value of five trials was calculated for each animal in different groups at seven days after MCAO before sacrifice.

#### *Tissue preparation*

At seven days after MCAO, eight rats from each group were randomly selected according to the table of random digit method to be sacrificed under deep anesthesia with 10% chloral hydrate (5 ml/kg body weight) and then transcardially perfused with 0.9% sodium chloride at 4°C followed by 4% paraformaldehyde in 0.1 M phosphate-buffer (PB, pH 7.4). The brains were then removed, kept in the same fixative for 4 h at 4°C and sequentially immersed in 20% and 30% sucrose in 0.1 M PB overnight at 4°C. Coronal sections were cut on a cryostat (CM1900; Leica) between +4.7 and -5.2 mm from bregma for histological analysis.

#### *Nissl staining*

A series of coronal sections in each animal between +4.7 and -5.2 mm from bregma were selected for Nissl staining to determine the volume of the primary infarction. Nissl staining was performed using 0.3% cresyl violet (860980; Sigma) and the images were captured with a camera and computer connected to the microscope (Olympus BX51; Tokyo). The primary cortical infarction volume was presented as a percentage of the contralateral hemisphere volume as previously described.<sup>14</sup>

#### *Immunofluorescent staining*

Coronal sections between -2.8 and -4.4 mm from bregma were selected to perform immunostaining.

Sections were blocked with 5% normal horse or goat serum and 0.1% Triton X-100 in 0.01 M PBS for 1 h at room temperature, and incubated with the following primary antibodies at 4°C overnight: mouse anti-BrdU (ab8152, Abcam), rabbit anti-rat laminin (L9393, Sigma-Aldrich), mouse anti-rat PECAM-1 (NB100-64796; Novus), rabbit anti-rat ephrinB2 (ab75868; Abcam), rabbit anti-rodent A $\beta$ <sub>3-16</sub> (SIG-39151; Covance), mouse anti-rat NeuN (ab104224; Abcam), mouse anti-rat GFAP (MAB3402X; Millipore), rabbit anti-rat Iba1 (019-19741; Wako) and rabbit anti-rat receptor for advanced glycation end product (RAGE; ab37647; Abcam). For BrdU double immunostaining, sections were treated with 2 N HCl for 30 min at 37°C and incubated in 0.1 M boric acid (pH 8.5) for 10 min at room temperature before being incubated in a blocking solution. Negative control sections were incubated with 0.01 M PBS rather than primary antibody. After being rinsed in 0.01 M PBS, sections were then incubated at room temperature for 1 h with secondary antibodies: Cy3-conjugated donkey anti-mouse IgG (715-166-150; Jackson ImmunoResearch Laboratories), FITC-conjugated goat anti-mouse IgG (115-096-003; Jackson ImmunoResearch Laboratories), FITC-conjugated goat anti-rabbit IgG (115-096-003; Jackson ImmunoResearch Laboratories) or Cy3-conjugated goat anti-rabbit IgG (111-166-003; Jackson ImmunoResearch Laboratories). Fluorescence signals were detected with a fluorescence microscope (Olympus BX51; Tokyo).

### Western blotting analysis

The rest four rats from each group were sacrificed at seven days after MCAO as described above and underwent intracardiac perfusion with 0.9% sodium chloride. The brain was removed and the ipsilateral and contralateral thalamus was separated. Total protein was extracted using Western blot lysis buffer with 1% protease inhibitor cocktail (Pierce) and the homogenate was centrifuged at 14,000  $\times g$  for 15 min at 4°C. Protein concentration was determined using the BCA protein assay system (Pierce). Eighty micrograms of protein extract from each sample were separated by SDS-PAGE gel electrophoresis and transferred to polyvinylidene fluoride membrane (Millipore). Non-specific binding was blocked with Tris-buffered saline containing 0.1% Tween-20 (TBST) and 5% nonfat milk (Sigma-Aldrich). The membranes were then incubated with primary antibodies as follows: rabbit polyclonal anti-ephrinB2 (ab75868; Abcam) and rabbit polyclonal anti-RAGE (ab37647; Abcam). The secondary antibodies were goat anti-rabbit IgG antibodies (7074; Cell Signaling Technology). The membranes were treated with a chemiluminescent system (7003; Cell

Signaling Technology) and then exposed with Kodak X-OMAT films.

### Image analysis and quantification

For quantitative analysis of immunostaining in the thalamus, every eighth section between  $-2.8$  and  $-4.4$  mm relative to bregma was randomly selected according to the table of random digit method by investigators blind to the treatment. The immunostaining positive cells were counted within three non-overlapping fields (400  $\times$  magnification) in the thalamus of each section using NIH Image software (Bethesda, Maryland). For quantification of A $\beta$  load in thalamus, the area of A $\beta$  fluorescence was analyzed as above and the percentage of thalamus region covered by A $\beta$  immunoreactivity was determined. For immunoblot, the relative densities of bands were quantified with the image analysis program as above, and the ratios of ephrinB2 and RAGE to GAPDH were calculated respectively.

### Statistical analysis

All data are expressed as median  $\pm$  interquartile range. Statistical analysis was conducted using Mann-Whitney test or Kruskal-Wallis ANOVA test for group comparisons. Differences were considered statistically significant at  $P < 0.05$ . Statistical analysis was performed using GraphPad Prism 6.0 software. Data analysis was performed in a blinder manner.

## Results

### Behavioral performance and cortical infarction

At seven days after MCAO, an increase in the mean time of adhesive-removal was observed in *Efnb2*-shRNA group when compared to the Scramble-shRNA group, trending towards significance ( $30.2 \pm 8.3$  vs.  $24.1 \pm 7.5$  s;  $P = 0.06$ ). However, EphB2-Fc treatment significantly accelerated the sensory recovery compared with those in the IgG-Fc group ( $14.2 \pm 9.1$  vs.  $27.0 \pm 10.3$  s;  $P < 0.05$ ). In addition, the relative infarct volumes were  $15.8 \pm 5.3\%$ ,  $15.4 \pm 3.4\%$ ,  $14.3 \pm 3.8\%$  and  $15.5 \pm 4.3\%$  in the Scramble-shRNA, *Efnb2*-shRNA, IgG-Fc and EphB2-Fc groups, respectively. There was no significant difference across various groups (all  $P > 0.05$ ).

### Cortical infarction stimulated angiogenesis in the ipsilateral thalamus

In the ipsilateral thalamus, BrdU<sup>+</sup>/laminin<sup>+</sup> cells were hardly observed in the sham-operated controls. In contrast, some BrdU-positive cell nuclei obviously were

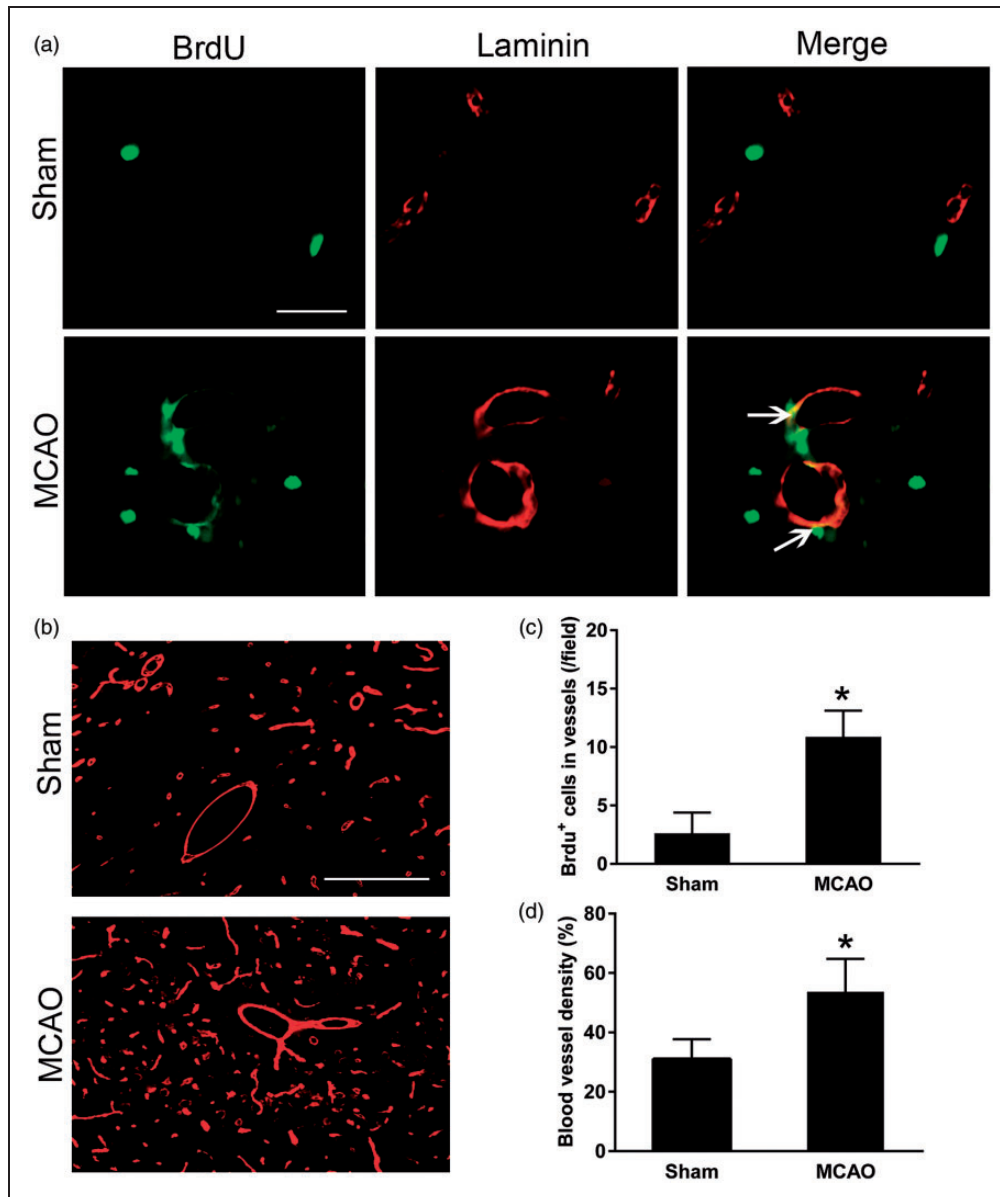


**Figure 1.** Enhanced angiogenesis in the ipsilateral thalamus after cortical infarction. (a) Immunostaining showing increased expression of BrdU<sup>+</sup> cells (green) in laminin-labelled blood vessels (red) in the ipsilateral thalamus at seven days after MCAO. Scale bar: 50  $\mu$ m. (b) Laminin-immunopositive blood vessels (red) within thalamus in sham-operated controls and ischemic group at seven days after MCAO. Scale bar: 100  $\mu$ m. (c and d) Quantitative analysis of number of BrdU<sup>+</sup> cells that co-stained for laminin and density of blood vessel.  $n = 8$ , data are expressed as median  $\pm$  interquartile range. \* $P < 0.05$  compared with the sham-operated controls.

co-localized with laminin-labeled cells within the ipsilateral thalamus at seven days after MCAO (Figure 1(a)). The number of BrdU<sup>+</sup>/laminin<sup>+</sup> cells was significantly increased within the ipsilateral thalamus at seven days after MCAO compared with the sham-operated group ( $P < 0.05$ , Figure 1(c)). In parallel, the density of laminin-labeled blood vessels in the ipsilateral thalamus of MCAO group was markedly higher than that in the sham-operated group ( $P < 0.05$ , Figure 1(b) and (d)). These results indicate

occurrence of angiogenesis in the ipsilateral thalamus after focal cerebral infarction.

#### *EphrinB2 knockdown reduced angiogenesis in the ipsilateral thalamus after cortical infarction*

The expression of ephrinB2 was significantly elevated within the ipsilateral thalamus at seven days after MCAO when compared to the sham-operated controls, and ephrinB2 immunostaining was mostly observed to

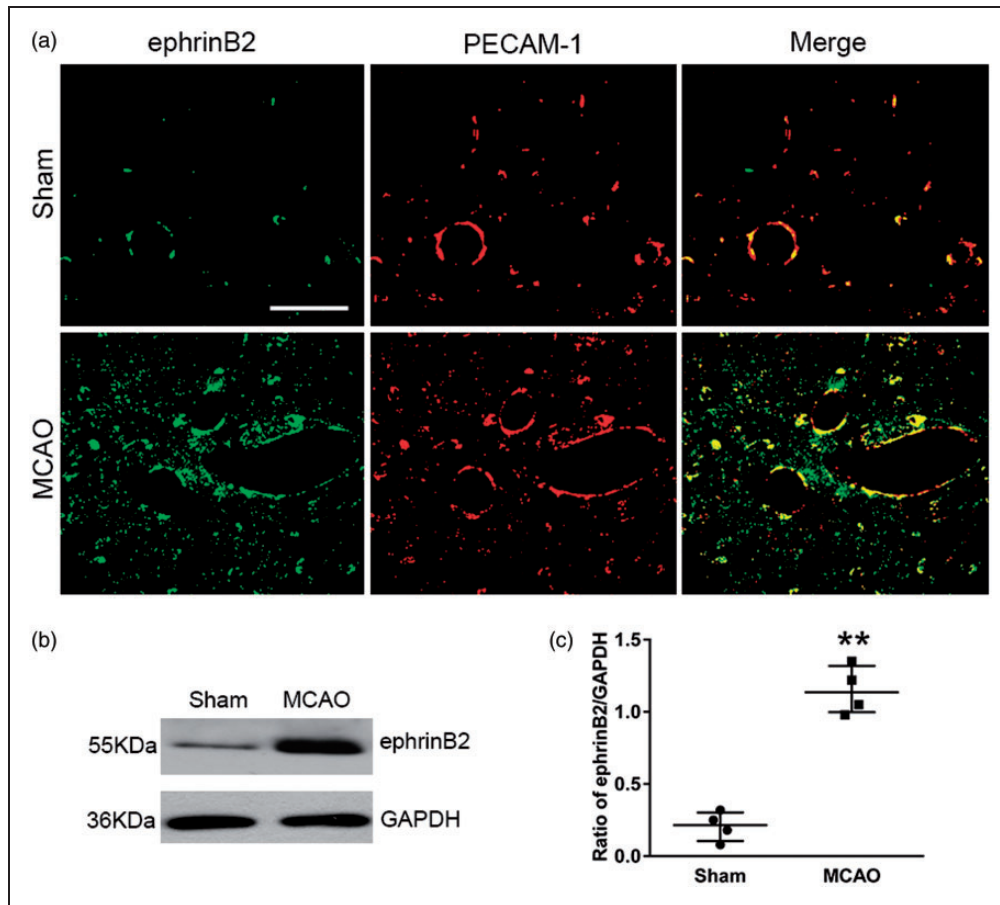


**Figure 2.** Expression of ephrinB2 in the ipsilateral thalamus after cortical infarction. (a) Cellular localization of ephrinB2 in the ipsilateral thalamus. Expression of ephrinB2 (green) that co-stained for PECAM-1 (red) was relatively low in the sham-operated thalamus. In contrast, ephrinB2/PECAM-1 double-staining markedly increased in the ipsilateral thalamus at seven days after MCAO. Scale bar: 50  $\mu$ m. (b) Immunoblot showing ephrinB2 levels in the thalamus of the sham-operated controls and post-MCAO group. (c) Quantitative analysis of ephrinB2 expression.  $n = 4$ , data are expressed as median  $\pm$  interquartile range.  $**P < 0.01$  compared with the sham-operated controls.

distribute in PECAM-1-immunoreactive blood vessels (Figure 2(a)). Immunoblotting revealed that the level of ephrinB2 significantly increased in the ipsilateral thalamus at seven days after MCAO, compared with that in the sham-operated controls ( $P < 0.01$ , Figure 2(b) and (c)), indicating the potential correlates of ephrinB2 with angiogenesis in the ipsilateral thalamus after cerebral infarction.

To determine the casual contribution of ephrinB2 to angiogenesis, *Efnb2*-shRNA or Scramble-shRNA was stereotactically injected into the right thalamus of hypertensive rats (Figure 3A(a)). GFP-tagged *Efnb2*-shRNA was dominantly observed within the ipsilateral thalamus at seven days post MCAO (Figure 3A(b)). Double immunofluorescence showed that GFP protein of *Efnb2*-shRNA or Scramble-shRNA was markedly colocalized with laminin-labeled endothelial cells within the ipsilateral thalamus at seven days after MCAO (Figure 3(B)). In addition,

ephrinB2-immunostaining was obviously decreased in the thalamus of the *Efnb2*-shRNA-treated group than those in the Scrambled-shRNA group (Figure 3(C)). Consistently, the levels of ephrinB2 within the ipsilateral thalamus of the *Efnb2*-shRNA group significantly reduced when compared to the Scramble-shRNA control group ( $P < 0.01$ , Figure 3(D) and (E)).

In parallel with reduction of ephrinB2, there were only few BrdU-positive cell nuclei to co-localize with laminin-labeled endothelial cells within the ipsilateral thalamus at seven days after MCAO (Figure 4(a)). Treatment with *Efnb2*-shRNA significantly decreased the number of BrdU<sup>+</sup>/laminin<sup>+</sup> cells within the ipsilateral thalamus at seven days after MCAO ( $P < 0.05$ , Figure 4(c)). In parallel, the density of laminin-labeled blood vessels in the ipsilateral thalamus of *Efnb2*-shRNA group was markedly lower than that in the group treated with Scramble-shRNA ( $P < 0.05$ , Figure 4(b) and (d)).

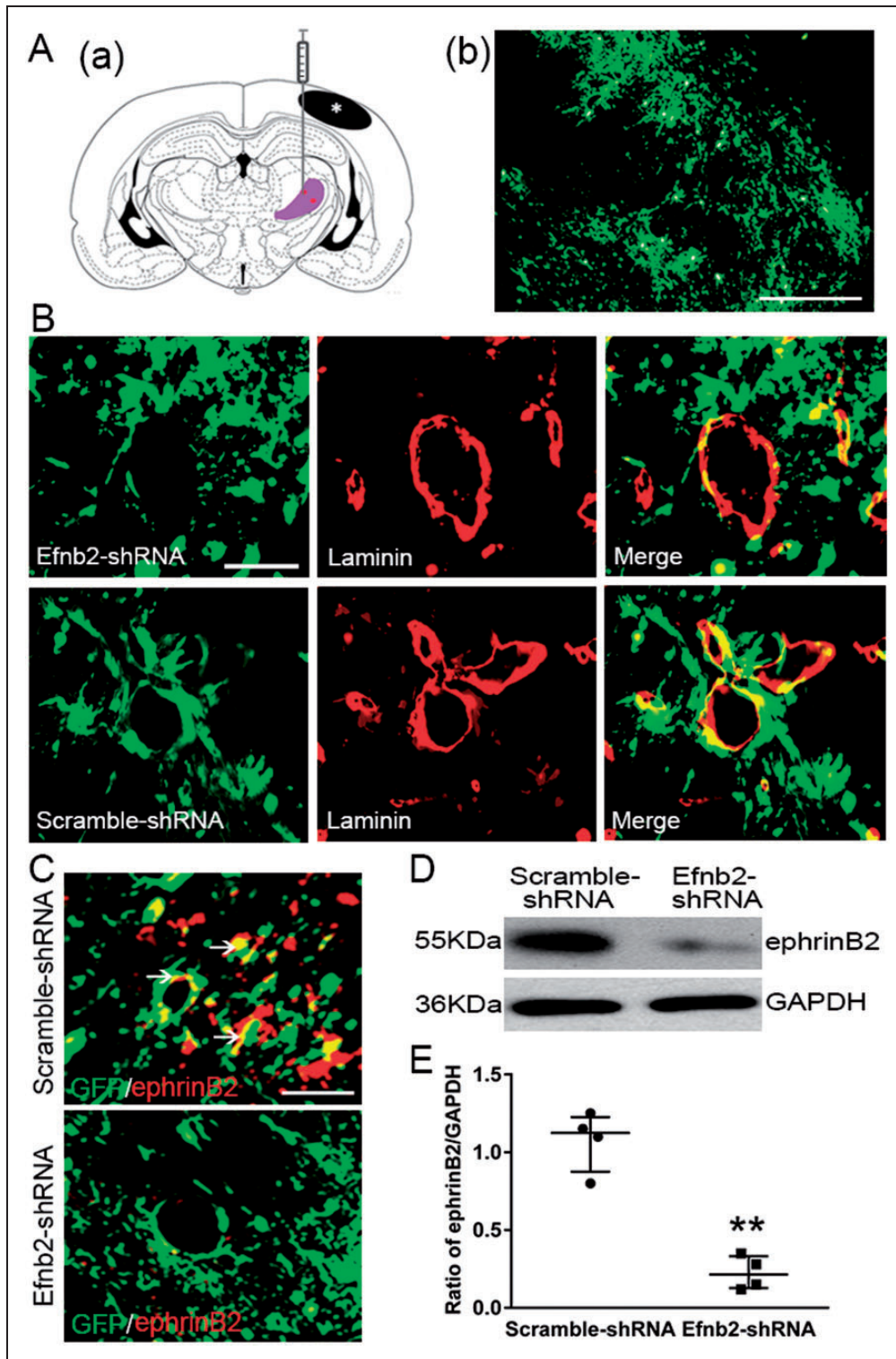


**Figure 3.** EphrinB2 knockdown by shRNA in the ipsilateral thalamus after cortical infarction. (Aa) Schematic diagram of brain section ( $-2.8$  mm from bregma) showing the location of cortical infarction (black color) and ipsilateral thalamus (purple color) where lentivirus was injected. (b) GFP-tagged shRNA was considerably detected in the thalamus at seven days after MCAO. (B) Immunoreactivity showing that GFP-tagged *Efnb2*-shRNA and Scramble-shRNA were expressed in laminin-immunopositive cells in the ipsilateral thalamus at seven days after MCAO. (C) Immunoreactivity showing co-staining of ephrinB2 with GFP-tagged shRNA. Scale bar: 50  $\mu$ m. (D) EphrinB2 knockdown markedly decreased ephrinB2 levels. (E) Quantitative analysis of ephrinB2 expression.  $n = 4$ , data are expressed as median  $\pm$  interquartile range. \*\* $P < 0.01$  compared with the Scramble-shRNA group.

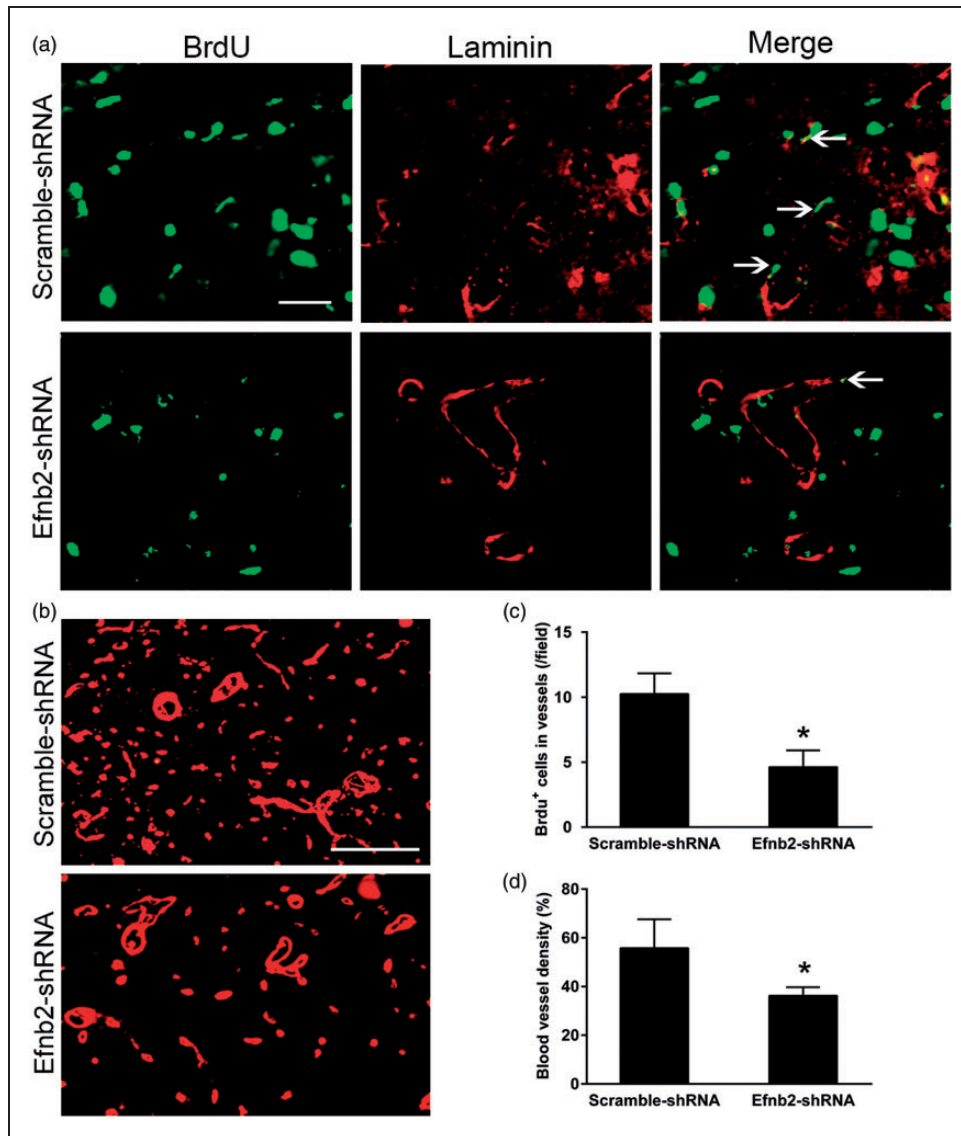


**Figure 4.** EphrinB2 knockdown and angiogenesis in the ipsilateral thalamus after cortical infarction. (a) Immunostaining for BrdU and laminin in the ipsilateral thalamus of the Scramble-shRNA and *Efnb2*-shRNA groups at seven days after MCAO. *Efnb2*-shRNA treatment markedly decreased BrdU<sup>+</sup> cells (green) that co-stained for laminin (red). Scale bar: 50  $\mu$ m. (b) Laminin-labeled blood vessel significantly decreased in the ipsilateral thalamus of the *Efnb2*-shRNA group at seven days after MCAO. (c and d) Quantitative analysis of the number of BrdU<sup>+</sup>/laminin<sup>+</sup> cells and density of blood vessel.  $n = 8$ , data are expressed as median  $\pm$  interquartile range. \* $P < 0.05$  compared with the Scramble-shRNA group.

#### Clustered EphB2-Fc enhanced angiogenesis in the ipsilateral thalamus after cortical infarction

To further confirm the contribution of ephrinB2 reverse molecular signaling to the angiogenesis within the ipsilateral thalamus, clustered EphB2-Fc was intraventricularly administered to activate ephrinB2.<sup>28,29</sup> Infusion of clustered EphB2-Fc significantly increased the number of BrdU<sup>+</sup>/laminin<sup>+</sup> cells within the ipsilateral thalamus compared with the IgG-Fc group at seven days after MCAO ( $P < 0.05$ , Figure 5(a) and (c)). Parallel to this, the density of laminin-labeled blood

vessels was obviously higher in the ipsilateral thalamus of EphB2-Fc group compared with that in the IgG-Fc group ( $P < 0.05$ , Figure 5(b) and (d)).

#### EphrinB2-induced angiogenesis was associated with A $\beta$ deposits and secondary damage in the ipsilateral thalamus after cortical infarction

We next examined whether ephrinB2-mediated angiogenesis regulated A $\beta$  deposits and the secondary neuronal damage in the thalamus. Immunostaining for A $\beta_{3-16}$  showed that there was extensive A $\beta$



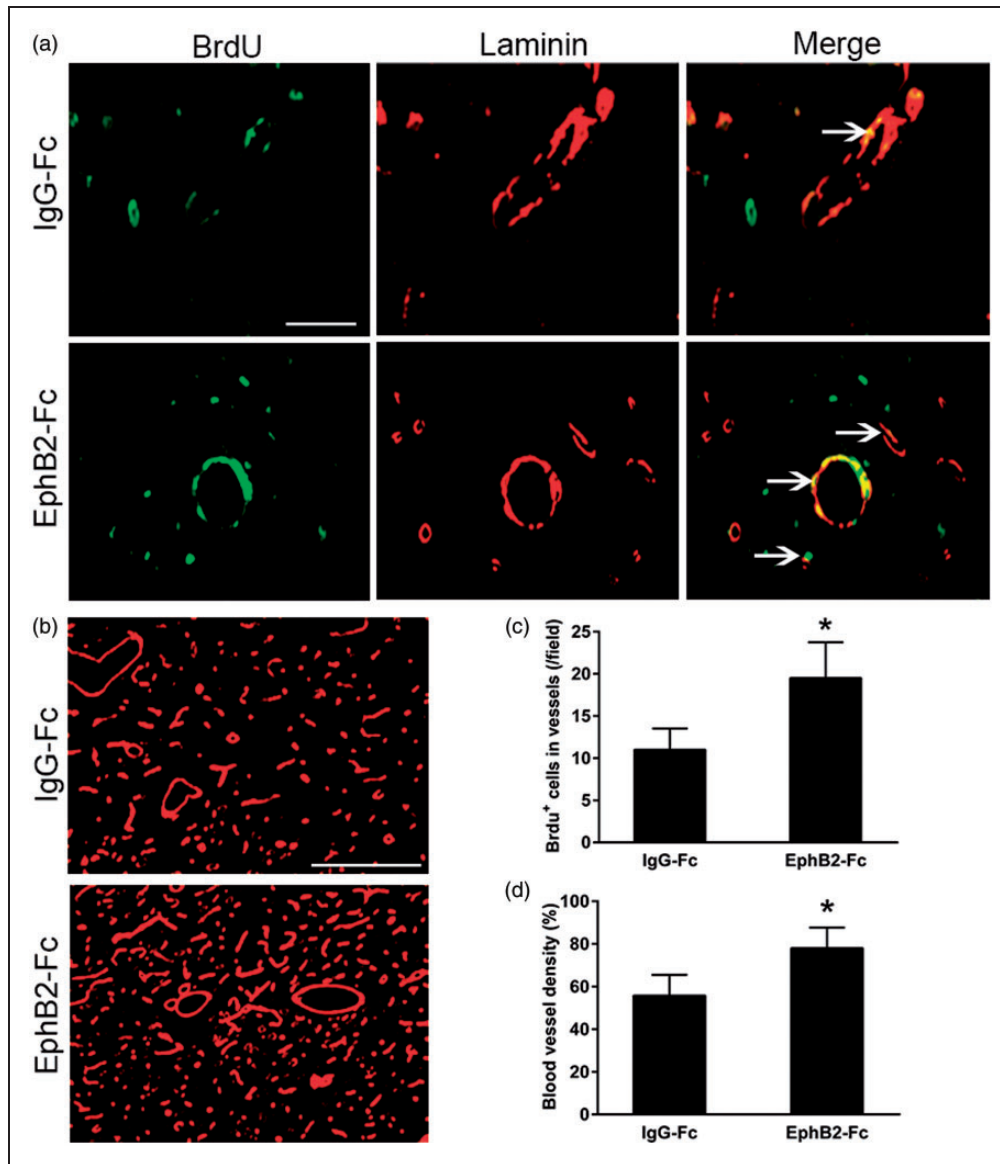


**Figure 5.** Clustered EphB2-Fc and angiogenesis in the ipsilateral thalamus after cortical infarction. (a) Immunostaining for BrdU and laminin in the ipsilateral thalamus of the IgG-Fc and EphB2-Fc groups at seven days after MCAO. EphB2-Fc infusion markedly increased BrdU<sup>+</sup> cells (green) that co-stained with laminin (red). Scale bar: 50  $\mu$ m. (b) Laminin-labeled blood vessel significantly increased in the ipsilateral thalamus of the EphB2-Fc group at seven days after MCAO. (c and d) Quantitative analysis of the number of BrdU<sup>+</sup>/laminin<sup>+</sup> cells and density of blood vessel.  $n = 8$ , data are expressed as median  $\pm$  interquartile range. \* $P < 0.05$  compared with the IgG-Fc group.

immunoreactivity in the ipsilateral thalamus in the Scramble-shRNA group at seven days after MCAO. Elevated A $\beta$  staining was observed in the ipsilateral thalamus of the *Efnb2*-shRNA group ( $P < 0.05$ ). In parallel, treatment with *Efnb2*-shRNA markedly decreased the number of NeuN<sup>+</sup> cells, while increased the number of GFAP<sup>+</sup> and Iba1<sup>+</sup> cells within the ipsilateral thalamus at seven days after MCAO (all  $P < 0.05$ ). In contrast, clustered EphB2-Fc infusion significantly reduced A $\beta$ , which was accompanied by increased NeuN<sup>+</sup> cells and decreased GFAP<sup>+</sup> and

Iba1<sup>+</sup> cells in the ipsilateral thalamus compared with the IgG-Fc group at seven days after MCAO (all  $P < 0.05$ , Figure 6(a) to (e)).

#### Activation of ephrinB2 altered RAGE expression in the ipsilateral thalamus after cortical infarction

RAGE has been shown to bind to the peripheral circulating A $\beta$  and mediates the influx of A $\beta$  across the blood-brain barrier.<sup>32</sup> We further explored the levels of RAGE across experimental groups. RAGE was

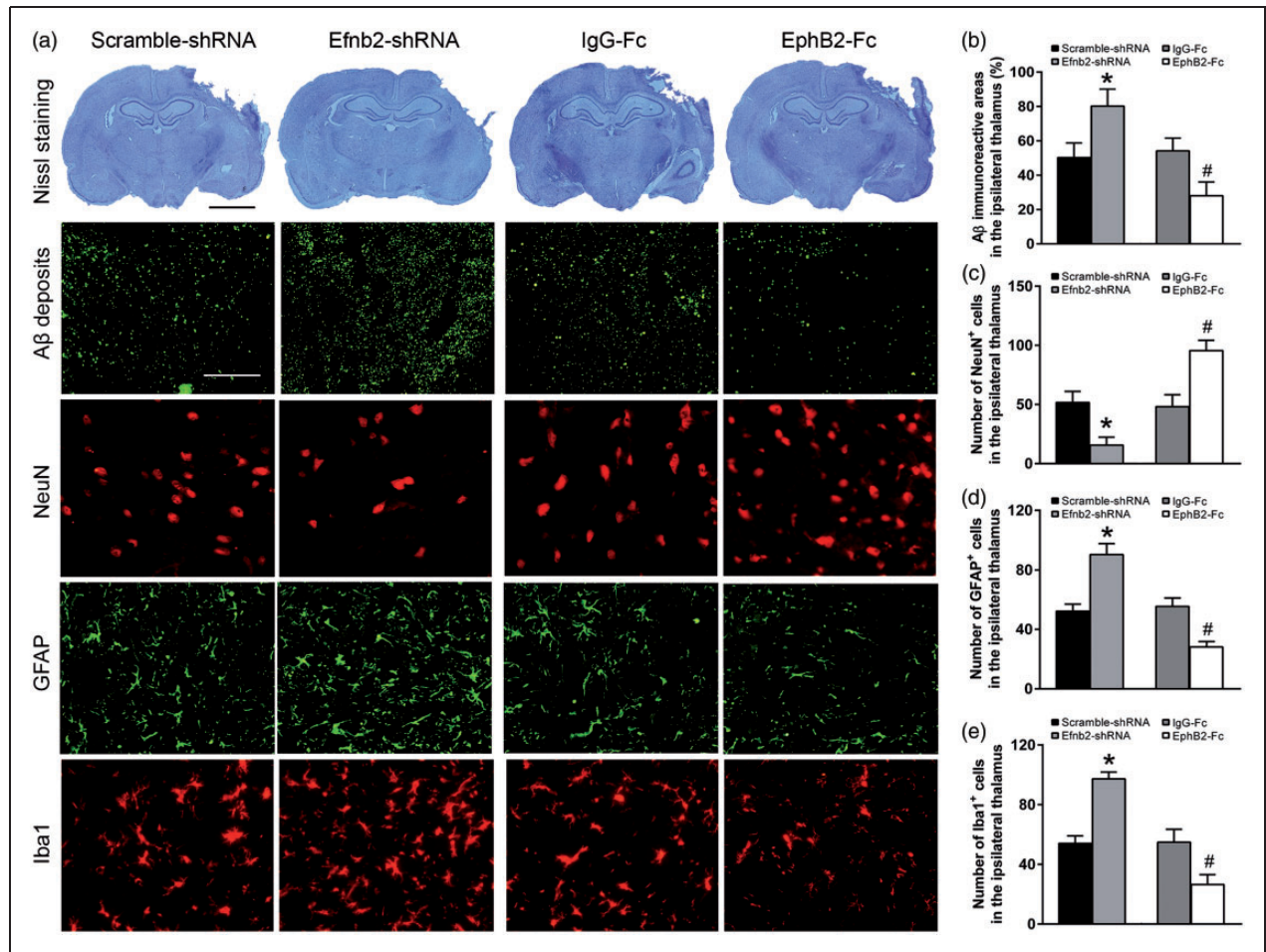


**Figure 6.** EphrinB2 activation and A $\beta$  deposits as well as secondary thalamic damage after cortical infarction. (a) Nissl staining showing cerebral infarction and immunostaining for A $\beta$ , NeuN, GFAP and Iba1 in the ipsilateral thalamus of the Scramble-shRNA, *Efnb2*-shRNA, IgG-Fc and EphB2-Fc groups at seven days after MCAO. *Efnb2*-shRNA treatment markedly increased A $\beta$  loads, the number of GFAP<sup>+</sup> and Iba1<sup>+</sup> cells, while decreased the number of NeuN<sup>+</sup> cells. In contrast, EphB2-Fc infusion decreased A $\beta$  loads, the number of GFAP<sup>+</sup> and Iba1<sup>+</sup> cells, whereas increased the number of NeuN<sup>+</sup> cells. Scale bar: 2 mm and 50  $\mu$ m. (b–e) Quantitative analysis of A $\beta$  loads, the number of NeuN<sup>+</sup>, GFAP<sup>+</sup> and Iba1<sup>+</sup> cells.  $n=8$ , data are expressed as median  $\pm$  interquartile range. \* $P < 0.05$  compared with the Scramble-shRNA group, # $P < 0.05$  compared with the IgG-Fc group.

observed to express on PECAM-1<sup>+</sup> endothelium within the ipsilateral thalamus at seven days after MCAO (Figure 7(a)). Immunoblotting further showed that RAGE level was significantly increased in ipsilateral thalamus of the *Efnb2*-shRNA group compared to the Scrambled-shRNA group ( $P < 0.05$ ). In contrast, clustered EphB2-Fc infusion markedly decreased the levels of RAGE in the ipsilateral thalamus compared to the IgG-Fc group ( $P < 0.05$ , Figure 7(b) and (c)), suggesting the activation of ephrinB2 might enhances A $\beta$  clearance through reducing RAGE expression.

## Discussion

The present study showed an elevated expression of ephrinB2 in the ipsilateral thalamus after focal cerebral infarction. Knockdown of ephrinB2 mediated by

siRNA markedly reduced angiogenesis, which was accompanied by increased A $\beta$  accumulation and the neuronal damage in the ipsilateral thalamus. In contrast, activation of ephrinB2 with EphB2-Fc enhanced angiogenesis and prevented A $\beta$  accumulation and the thalamic damage. This effect was correlated with an accelerated functional recovery. Furthermore, knockdown of ephrinB2 significantly increased endothelial RAGE expression, whereas activation of ephrinB2 markedly decreased levels of RAGE. Taken together, our findings suggest that ephrinB2-mediated angiogenesis ameliorates A $\beta$  accumulation and the secondary neurodegeneration in the thalamus at an early stage after focal cerebral infarction. In addition, RAGE might be involved in A $\beta$  metabolism in the thalamus.

In agreement with previous studies,<sup>13–15</sup> we showed that BrdU/laminin double-positive cells and

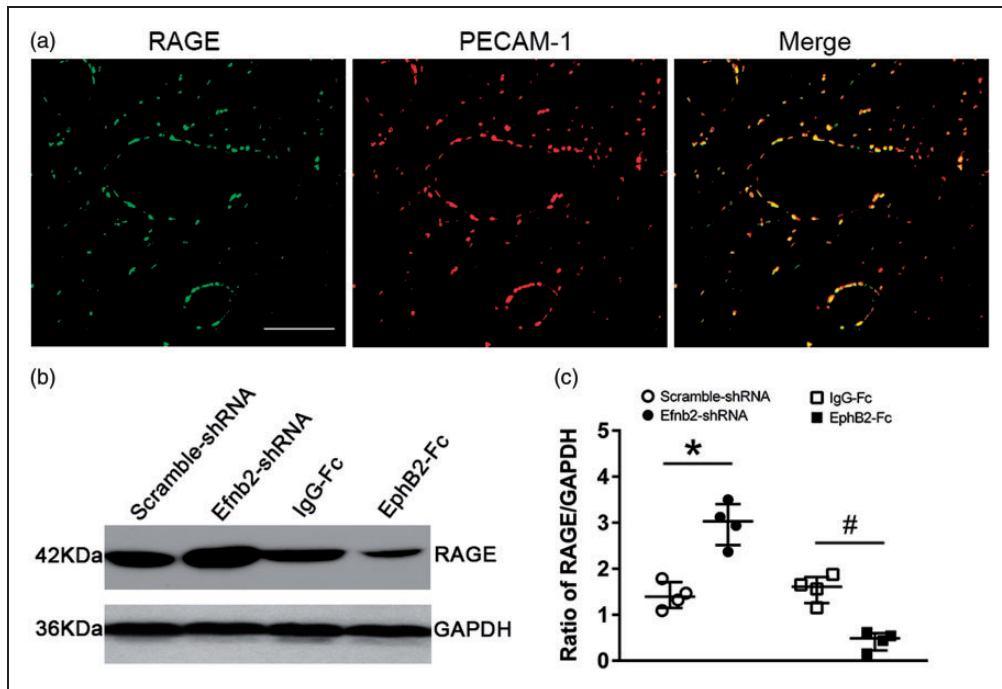


**Figure 7.** EphrinB2 activation and RAGE expression in the ipsilateral thalamus after cortical infarction. (a) Co-staining of RAGE (green) and PECAM-1 (red) in the ipsilateral thalamus at seven days after MCAO. Scale bar: 50  $\mu$ m. (b) *Efnb2*-shRNA treatment markedly increased RAGE levels, whereas EphB2-Fc infusion decreased RAGE expression in the ipsilateral thalamus at seven days after MCAO. (c) Quantitative analysis of RAGE levels.  $n = 4$ , data are expressed as median  $\pm$  interquartile range. \* $P < 0.05$  compared with the Scramble-shRNA group, # $P < 0.05$  compared with the IgG-Fc group.

laminin-labeled vascular density were markedly increased in the ipsilateral thalamus at seven days after focal cerebral infarction, suggesting the occurrence of angiogenesis at an early stage after cerebral infarction. However, the molecular mechanisms underlying angiogenesis in thalamus had not yet been identified. Recent studies have shown that increased expression of ephrinB2 enhanced the vessel remodeling after hind limb ischemia and ischemic cardiovascular disease.<sup>33,34</sup> More recently, ephrinB2 has been found to be upregulated in peri-infarct brain regions within three days after injury and activation of ephrinB2 by EphB4 promotes the vascular repair mechanism after mild ischemic stroke.<sup>35</sup> In the present study, we found ephrinB2 to be upregulated on endothelial cells in parallel with angiogenesis within the non-ischemic thalamus even at seven days after cerebral cortical infarction. These observations led us to hypothesize that ephrinB2 signaling might be involved in post-stroke angiogenesis in the thalamus. Our results showed that siRNA-mediated downregulation of ephrinB2 significantly reduced the number of BrdU/laminin double-positive cells and the vascular density within the ipsilateral thalamus after cerebral cortical infarction, indicating blocking ephrinB2 signaling inhibits angiogenesis in the thalamus. Next, we explore whether activation of ephrinB2 signaling enhances

angiogenesis in the thalamus. It has been shown that ephrinB2 and EphB2 expressed on pericytes adjacent to endothelial cells contribute to angiogenesis.<sup>20</sup> Furthermore, clustered EphB2-Fc can activate its cognate ephrinB2 reversal signaling.<sup>28–30</sup> We then examined the effects of activating ephrinB2 by infusion of recombinant EphB2-Fc on angiogenesis. Our results showed that activation of ephrinB2 by EphB2-Fc markedly enhanced the angiogenesis within the ipsilateral thalamus as evidenced by increased BrdU/laminin-positive cells and blood vessel density, suggesting the involvement of ephrinB2 in angiogenesis in the thalamus at an early stage after cerebral cortical infarction.

Epidemiological studies show that ischemic stroke markedly increases the risk of AD and contributes to the incidence of AD in patients with mild cognitive decline,<sup>36–38</sup> suggesting a close relationship between ischemic stroke and AD. Consistently, neuronal damage and A $\beta$  accumulation in the ipsilateral thalamus are evident following experimental stroke,<sup>7,9,10</sup> whereas blockade of A $\beta$  production can reduce the neuronal injury in thalamus following ischemic stroke,<sup>12</sup> indicating the direct interaction between thalamic damage after ischemic stroke and A $\beta$  accumulation. Interestingly, recent studies have demonstrated that induction of angiogenesis can ameliorate A $\beta$  accumulation in experimental models of AD.<sup>39,40</sup> Based on

these findings, we supposed that promotions of angiogenesis in the thalamus could eliminate A $\beta$  accumulation and then rescue the neuronal damage of thalamus after cerebral infarction. Here, we found that inhibition of angiogenesis by siRNA-mediated knockdown of ephrinB2 resulted in marked A $\beta$  accumulation, whereas enhanced angiogenesis by EphB2-Fc markedly decreased A $\beta$  loads in the thalamus. Furthermore, these effects were associated with better functional recovery in parallel with restoration of thalamic neural damage including reduction of neuron loss and reactive astrocytes and microglia. The mechanism of A $\beta$  pathology in the thalamus is unclear. Previous studies have suggested that RAGE, one endothelial transporter, mediates the influx of vascular A $\beta$  and facilitates clearance of A $\beta$  in AD brain.<sup>41</sup> Reduction of endothelial RAGE levels ameliorates A $\beta$  loads in brain of AD model.<sup>40</sup> Consistently, we found that enhanced angiogenesis by activating ephrinB2 coincided in decreased RAGE expression in the thalamus after cortical infarction, suggesting a possible role of RAGE in clearance of A $\beta$  under the current circumstance. Taken together, the present results indicate a protective role of ephrinB2-mediated angiogenesis in thalamic pathology secondary to cerebral infarction.

In addition to endothelial cells, ephrinB2 is also expressed on several other types of cells including astrocytes, microglia and neurons.<sup>30,35</sup> Therefore, we could not rule out the involvement of these cell types in ephrinB2-mediated actions. Activated astrocytes or microglia have been shown to increase the production of A $\beta$  in AD brain.<sup>42,43</sup> Furthermore, A $\beta$  accumulation also causes astrocyte and microglia activation.<sup>44</sup> Our results showed that reactive astrocytes and microglia were correlated with an increase in A $\beta$  accumulation, whereas activation of ephrinB2 reduced A $\beta$  accumulation and inhibited activation of astrocytes and microglia, suggesting a possible interaction between the astrocytic and microglial response and A $\beta$  accumulation. Alternatively, the reactive gliosis may principally represent a glial response to the neural injury as seen in the brain of stroke and AD.<sup>27,45</sup> The close correlates of gliosis and neuron loss might be indicative of exaggerated neurodegeneration in the ipsilateral thalamus after ephrinB2 knockdown. Interestingly, one recent study has proposed the plausible action of ephrinB2 on the pathogenesis of AD. In presenilin1 (PS1)-knockout mice, PS1 mutants inhibited the function of ephrinB2 reversal signaling, thereby contributing to the pathological changes in the brain of AD.<sup>46</sup> Nevertheless, the direct actions of ephrinB2 on different cell types under the current circumstance need further elucidation.

Several limitations should be noted in the present study. Firstly, our findings provide insights into the

actions of ephrinB2 on the secondary thalamic damage and functional recovery at the early stage after cerebral infarction. However, we were unable to clarify the long-term effects of ephrinB2 signaling on both functional and pathological outcomes. Secondly, it remains unclear how reciprocal communication between cells expressing ephrinB2 and its Eph receptors modulates the vessel remodeling in the thalamus. Further study needs to elucidate the exact mechanisms of ephrinB2/Ephs signaling system involved in angiogenesis in the thalamus after cerebral infarction.

## Conclusions

In summary, our findings demonstrate that activation of ephrinB2 can promote angiogenesis, decrease A $\beta$  deposits and rescue the secondary neurodegeneration of thalamus after cerebral infarction. Thus, specific stimulation of ephrinB2 might be a novel strategy to promote angiogenesis and rescue the thalamic degeneration secondary to cerebral infarction.

## Funding

The author(s) disclosed receipt of the following financial support for the research, authorship, and/or publication of this article: the National Key R&D Program of China (2017YFC1307500), the National Natural Science Foundation of China (81000500), the Natural Science Foundation of Guangdong Province of China (2015A030313049, 2017A030303011), the Science and Technology Planning Project of Guangdong Province of China (2017A050506024), the National Key Clinical Department, National Key Discipline, the Guangdong Provincial Key Laboratory for diagnosis and treatment of major neurological diseases (2014B030301035) and the Southern China International Cooperation Base for Early Intervention and Functional Rehabilitation of Neurological Diseases (2015B050501003).

## Declaration of conflicting interests

The author(s) declared no potential conflicts of interest with respect to the research, authorship, and/or publication of this article.

## Authors' contributions

SHX conceived the study and drafted the manuscript, JJJ, JZ, NNP and WX conducted the experiment, CD and GL contributed to the analysis of the data, ZP and JSZ contributed to the data interpretation and editing of the manuscript. All authors contributed to editing of the manuscript.

## References

1. Iizuka H, Sakatani K and Young W. Neural damage in the rat thalamus after cortical infarcts. *Stroke* 1990; 21: 790–794.

2. Tamura A, Tahira Y, Nagashima H, et al. Thalamic atrophy following cerebral infarction in the territory of the middle cerebral artery. *Stroke* 1991; 22: 615–618.
3. Block F, Dihne M and Loos M. Inflammation in areas of remote changes following focal brain lesion. *Prog Neurobiol* 2005; 75: 342–365.
4. He M, Xing S, Yang B, et al. Ebselen attenuates oxidative DNA damage and enhances its repair activity in the thalamus after focal cortical infarction in hypertensive rats. *Brain Res* 2007; 1181: 83–92.
5. Wang F, Liang Z, Hou Q, et al. Nogo-A is involved in secondary axonal degeneration of thalamus in hypertensive rats with focal cortical infarction. *Neurosci Lett* 2007; 417: 255–260.
6. Uchino A, Sawada A, Takase Y, et al. Transient detection of early wallerian degeneration on diffusion-weighted MRI after an acute cerebrovascular accident. *Neuroradiology* 2004; 46: 183–188.
7. Mäkinen S, van Groen T, Clarke J, et al. Coaccumulation of calcium and beta-amyloid in the thalamus after transient middle cerebral artery occlusion in rats. *J Cereb Blood Flow Metab* 2008; 28: 263–268.
8. Hiltunen M, Mäkinen P, Peraniemi S, et al. Focal cerebral ischemia in rats alters APP processing and expression of Abeta peptide degrading enzymes in the thalamus. *Neurobiol Dis* 2009; 35: 103–113.
9. van Groen T, Puurunen K, Mäki HM, et al. Transformation of diffuse beta-amyloid precursor protein and beta-amyloid deposits to plaques in the thalamus after transient occlusion of the middle cerebral artery in rats. *Stroke* 2005; 36: 1551–1556.
10. Ong LK, Zhao Z, Kluge M, et al. Chronic stress exposure following photothrombotic stroke is associated with increased levels of Amyloid beta accumulation and altered oligomerisation at sites of thalamic secondary neurodegeneration in mice. *J Cereb Blood Flow Metab* 2017; 37: 1338–1348.
11. Zhang J, Zhang Y, Li J, et al. Autophagosomes accumulation is associated with beta-amyloid deposits and secondary damage in the thalamus after focal cortical infarction in hypertensive rats. *J Neurochem* 2012; 120: 564–573.
12. Zhang Y, Xing S, Zhang J, et al. Reduction of beta-amyloid deposits by gamma-secretase inhibitor is associated with the attenuation of secondary damage in the ipsilateral thalamus and sensory functional improvement after focal cortical infarction in hypertensive rats. *J Cereb Blood Flow Metab* 2011; 31: 572–579.
13. Beck H and Plate KH. Angiogenesis after cerebral ischemia. *Acta Neuropathol* 2009; 117: 481–496.
14. Ling L, Zeng J, Pei Z, et al. Neurogenesis and angiogenesis within the ipsilateral thalamus with secondary damage after focal cortical infarction in hypertensive rats. *J Cereb Blood Flow Metab* 2009; 29: 1538–1546.
15. Hayward NM, Yanev P, Haapasalo A, et al. Chronic hyperperfusion and angiogenesis follow subacute hypoperfusion in the thalamus of rats with focal cerebral ischemia. *J Cereb Blood Flow Metab* 2011; 31: 1119–1132.
16. Zlokovic BV. Neurovascular pathways to neurodegeneration in Alzheimer's disease and other disorders. *Nat Rev Neurosci* 2011; 12: 723–738.
17. Davy A and Soriano P. Ephrin signaling in vivo: look both ways. *Dev Dyn* 2005; 232: 1–10.
18. Wang HU, Chen ZF and Anderson DJ. Molecular distinction and angiogenic interaction between embryonic arteries and veins revealed by ephrin-B2 and its receptor Eph-B4. *Cell* 1998; 93: 741–753.
19. Gerety SS, Wang HU, Chen ZF, et al. Symmetrical mutant phenotypes of the receptor EphB4 and its specific transmembrane ligand ephrin-B2 in cardiovascular development. *Mol Cell* 1999; 4: 403–414.
20. Adams RH, Wilkinson GA, Weiss C, et al. Roles of ephrinB ligands and EphB receptors in cardiovascular development: demarcation of arterial/venous domains, vascular morphogenesis, and sprouting angiogenesis. *Genes Dev* 1999; 13: 295–306.
21. Adams RH, Diella F, Hennig S, et al. The cytoplasmic domain of the ligand ephrinB2 is required for vascular morphogenesis but not cranial neural crest migration. *Cell* 2001; 104: 57–69.
22. Hayashi S, Asahara T, Masuda H, et al. Functional ephrin-B2 expression for promotive interaction between arterial and venous vessels in postnatal neovascularization. *Circulation* 2005; 111: 2210–2218.
23. Salvucci O, Ohnuki H, Maric D, et al. EphrinB2 controls vessel pruning through STAT1-JNK3 signalling. *Nat Commun* 2015; 6: 6576.
24. Foo SS, Turner CJ, Adams S, et al. Ephrin-B2 controls cell motility and adhesion during blood-vessel-wall assembly. *Cell* 2006; 124: 161–173.
25. Zeng J, Zhang Y, Mo J, et al. Two-kidney, two clip renovascular hypertensive rats can be used as stroke-prone rats. *Stroke* 1998; 29: 1708–1713.
26. Brint S, Jacewicz M, Kiessling M, et al. Focal brain ischemia in the rat: methods for reproducible neocortical infarction using tandem occlusion of the distal middle cerebral and ipsilateral common carotid arteries. *J Cereb Blood Flow Metab* 1988; 8: 474–485.
27. Xing S, Zhang Y, Li J, et al. Beclin 1 knockdown inhibits autophagic activation and prevents the secondary neurodegenerative damage in the ipsilateral thalamus following focal cerebral infarction. *Autophagy* 2012; 8: 63–76.
28. Dong LD, Gao F, Wang XH, et al. GluA2 trafficking is involved in apoptosis of retinal ganglion cells induced by activation of EphB/EphrinB reverse signaling in a rat chronic ocular hypertension model. *J Neurosci* 2015; 35: 5409–5421.
29. Ethell IM, Irie F, Kalo MS, et al. EphB/syndecan-2 signaling in dendritic spine morphogenesis. *Neuron* 2001; 31: 1001–1013.
30. Conover JC, Doetsch F, Garcia-Verdugo JM, et al. Disruption of Eph/ephrin signaling affects migration and proliferation in the adult subventricular zone. *Nat Neurosci* 2000; 3: 1091–1097.
31. Schallert T, Upchurch M, Wilcox RE, et al. Posture-independent sensorimotor analysis of inter-hemispheric receptor asymmetries in neostriatum. *Pharmacol Biochem Behav* 1983; 18: 753–759.

32. Deane R, Du Yan S, Subramanian RK, et al. RAGE mediates amyloid-beta peptide transport across the blood-brain barrier and accumulation in brain. *Nat Med* 2003; 9: 907–913.
33. Yang D, Jin C, Ma H, et al. EphrinB2/EphB4 pathway in postnatal angiogenesis: a potential therapeutic target for ischemic cardiovascular disease. *Angiogenesis* 2016; 19: 297–309.
34. Katsu M, Koyama H, Maekawa H, et al. Ex vivo gene delivery of ephrin-B2 induces development of functional collateral vessels in a rabbit model of hind limb ischemia. *J Vasc Surg* 2009; 49: 192–198.
35. Ghori A, Freimann FB, Nieminen-Kelha M, et al. EphrinB2 activation enhances vascular repair mechanisms and reduces brain swelling after mild cerebral ischemia. *Arterioscler Thromb Vasc Biol* 2017; 37: 867–878.
36. Desmond DW, Moroney JT, Sano M, et al. Incidence of dementia after ischemic stroke: results of a longitudinal study. *Stroke* 2002; 33: 2254–2260.
37. Reitz C, Brayne C and Mayeux R. Epidemiology of Alzheimer disease. *Nat Rev Neurol* 2011; 7: 137–152.
38. Thiel A, Cechetto DF, Heiss WD, et al. Amyloid burden, neuroinflammation, and links to cognitive decline after ischemic stroke. *Stroke* 2014; 45: 2825–2829.
39. Koster KP, Thomas R, Morris AW, et al. Epidermal growth factor prevents oligomeric amyloid-beta induced angiogenesis deficits in vitro. *J Cereb Blood Flow Metab* 2016; 36: 1865–1871.
40. Lee ST, Chu K, Park JE, et al. Erythropoietin improves memory function with reducing endothelial dysfunction and amyloid-beta burden in Alzheimer's disease models. *J Neurochem* 2012; 120: 115–124.
41. Yan SD, Chen X, Fu J, et al. RAGE and amyloid-beta peptide neurotoxicity in Alzheimer's disease. *Nature* 1996; 382: 685–691.
42. Zhao J, O'Connor T and Vassar R. The contribution of activated astrocytes to Abeta production: implications for Alzheimer's disease pathogenesis. *J Neuroinflammation* 2011; 8: 150.
43. Lian H, Litvinchuk A, Chiang AC, et al. Astrocyte-microglia cross talk through complement activation modulates amyloid pathology in mouse models of Alzheimer's disease. *J Neurosci* 2016; 36: 577–589.
44. White JA, Manelli AM, Holmberg KH, et al. Differential effects of oligomeric and fibrillar amyloid-beta 1-42 on astrocyte-mediated inflammation. *Neurobiol Dis* 2005; 18: 459–465.
45. Pike CJ, Cummings BJ and Cotman CW. Early association of reactive astrocytes with senile plaques in Alzheimer's disease. *Exp Neurol* 1995; 132: 172–199.
46. Georgakopoulos A, Xu J, Xu C, et al. Presenilin1/gamma-secretase promotes the EphB2-induced phosphorylation of ephrinB2 by regulating phosphoprotein associated with glycosphingolipid-enriched microdomains/Csk binding protein. *FASEB J* 2011; 25: 3594–3604.